J Mater Sci (2011) 46:7850–7857
DOI 10.1007/s10853-011-5766-3

Compressive mechanical properties and deformation behavior of porous polymer blends of poly(ε-caprolactone) and poly(L-lactic acid)

Joo-Eon Park · Mitsugu Todo

Received: 23 March 2011 / Accepted: 1 July 2011 / Published online: 15 July 2011

Abstract Porous biodegradable polymeric scaffolds are developed by physically blending two different kinds of biodegradable polymers, PCL, and PLLA, for application in tissue engineering. The main objective of the development of this material is to control the mechanical properties, such as, elastic modulus and strength. The results from mechanical testing showed that the compressive mechanical properties of PCL/PLLA scaffold can be varied by changing the blend ratio. It also showed that these properties can be well predicted by the rule of mixture. The primary deformation mechanism of the scaffolds was found to be localized buckling of struts surrounding the pores. Localized ductile failure caused by PCL phase tends to be suppressed with increasing PLLA content. The immiscibility of PCL and PLLA caused the phase-separation morphology that strongly affected the macroscopic mechanical properties and the microscopic deformation behavior.

Introduction

In the tissue engineering field, various types of three-dimensional porous structures have been developed as scaffolds for regenerating different types of tissues such as, bone, cartilage, vasculature, ligament, nerve, and skin [1–12]. The scaffolds with target cells or regenerated tissues are implanted into the corresponding damaged tissues for regeneration. For a successful regeneration to occur, the scaffold needs to have suitable mechanical properties and porous structure, until the seeded cells or the regenerated tissues become adapted to the surrounding environment. If the scaffold has much lower mechanical properties than the surrounding tissue, the scaffold could severely deform or fracture, and tissue regeneration will not occur. It is therefore important to develop the scaffolds with controllable mechanical properties and with suitable porous structures to ensure the mechanical stability with sufficient tissue growth during the regeneration process.

In recent years, biodegradable thermoplastic polymers such as, poly(ε-caprolactone) (PCL) and poly(L-lactic acid) (PLLA) have been used for scaffolds, mainly owing to their biocompatibility, bioabsorbability, and reasonable mechanical properties [13–21]. It is known that, PCL has much lower mechanical properties with higher ductility than the brittle PLLA, while PLLA has the properties comparable to engineering plastics. By blending these two polymers, a material with controlled mechanical properties can be developed [22–24].

In the present study, porous PCL/PLLA polymer blends were developed with various compressive mechanical properties by controlling the blend ratio. Solid–liquid-phase separation and freeze-drying methods [25, 26] were utilized to fabricate the porous structures. Effects of the PLLA content on the mechanical properties were examined and simple theoretical analyses were conducted to predict the experimental values. The microstructure and deformation behavior at the critical points were also characterized by using a field emission-scanning electron microscope (FE-SEM). A differential scanning calorimeter (DSC) was also used to characterize the thermal properties.

J.-E. Park
Interdisciplinary Graduate School of Engineering Sciences, Kyushu University, 6-1 Kasuga-koen, Kasuga 816-8580, Japan

M. Todo (✉)
Research Institute for Applied Mechanics, Kyushu University, 6-1 Kasuga-koen, Kasuga 816-8580, Japan
e-mail: todo@riam.kyushu-u.ac.jp

Experiment

Materials and specimen preparation

PCL (CelgreenH7, Daicel, Chemistry Industries Co.) and PLLA pellets (Lacty#5000, Shimadzu Co., Ltd) were used to fabricate porous PCL/PLLA scaffold specimens. The material properties of PCL and PLLA polymers are summarized in Table 1. The solid–liquid-phase separation and freeze-drying methods were utilized to fabricate the porous structures. The schematic procedure of the fabrication process is illustrated in Fig. 1. PCL and PLLA pellets were first dissolved in a solvent, 1,4-dioxane, and the concentration of the mixed polymer blends was kept at 7 wt% in solution. The chosen blend ratios were PCL/PLLA = 70:30, 50:50, and 20:80. Pure PCL and PLLA scaffolds were also fabricated for comparison. These mixed polymer solutions were filled in PP tubes and frozen by immersing them into liquid nitrogen from the bottom at a constant rate. The difference in the freezing behavior of the solute- and the solvent-induced-phase separation and resulted in the porous nature of the solute. The solidified PCL/PLLA blends were then dried under vacuum at −5 °C for about 1 week to create the porous structure.

Cylindrical stick-type scaffold specimens of 8.5 mm diameter were obtained and cut into disk specimens of 11 mm length for compression test as shown in Fig. 2. (From hereafter, the PCL/PLLA scaffold specimen will be denoted as PCPL.)

Table 1 Material properties of PCL and PLLA polymer

Polymer	Average Mw/10^5 (g/mol)	Density at room temp. (g/cm^3)	Glass transition temp. (°C)	Melting temp. (°C)
PCL	5.3	1.095	−60.55	63.73
PLLA	3.51	1.248	69.72	174.9

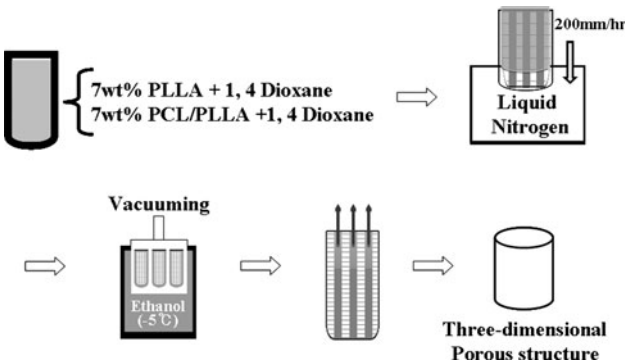

Fig. 1 Schematic procedure of scaffold preparation

Porosity and microstructural characterization

The porosity of a scaffold, $\varepsilon_{\text{porosity}}$, was estimated by the following formula:

$$\varepsilon_{\text{porosity}} = \frac{V_{\text{total}} - V_{\text{polymer}}}{V_{\text{total}}} \times 100 \quad (1)$$

where, V_{total} is the measured volume of the scaffold specimen and V_{polymer} is the actual volume of the polymer solid within the scaffold. Therefore, $(V_{\text{total}} - V_{\text{polymer}})$ denotes the volume of the pores.

The microstructures of the scaffolds were characterized by observing the longitudinal and the horizontal cross-sections using FE-SEM (S-4100, Hitachi, Japan). The vertical cross-sections were obtained by cutting the specimens along the central line by flesh razor blades after being frozen in liquid nitrogen for several minutes. The samples were then placed on aluminum disks and were coated with *Pt–Pd* on the entire cutting surfaces by using an Ion sputter coater (E-1030, Hitachi, Japan). The coated surfaces were then observed using FE-SEM.

The morphology of phase separation of PCL/PLLA blends was also characterized by observing the microstructures of blend films obtained by the solution casting. Small portions of the PCPL scaffolds were dissolved in 1,4-dioxane and poured into plastic cases. After the dioxane solvent completely evaporated, film-like structures were obtained. The surface morphology of the films was then observed by FE-SEM to characterize the phase separation.

Thermal analysis

Thermal properties such as, glass transition and melting temperatures were determined by using a differential scanning calorimeter (DSC, DSC-60A, Shimadzu Corp.). For the DSC analysis, sample sizes ranging from 4 to 6 mg were selected and put into an aluminum container with a cover. PCL/PLLA blend samples were cooled to −100 °C

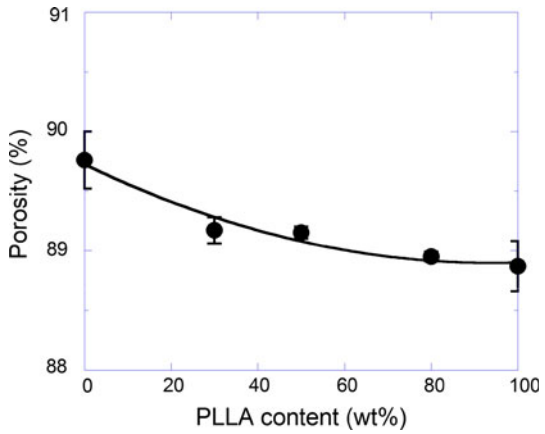

Fig. 2 Effect of PLLA content on porosity

and then heated up to 230 °C under nitrogen gas flow at a rate of 10 °C/min, and the melting curves were recorded. For pure PLLA and PCL samples, DSC analysis was performed from 40 to 230 °C and −100 to 230 °C, respectively.

Crystallinities of PLLA, $x_{c.PLLA}$, in the pure and blend samples, were evaluated using the following equations [27]:

$$x_{c.PLLA}(\%) = \frac{100 \times (dH_{m.PLLA} + dH_{c.PLLA})}{135 \times (1 - X) \times X_{PLLA}} \quad (2)$$

$$x_{c.PCL}(\%) = \frac{100 \times (dH_{m.PCL})}{142 \times (1 - X) \times (1 - X_{PLLA})} \quad (3)$$

$$X_{PLLA} = \frac{W_{PLLA}}{W_{PLLA} + W_{PCL}} \quad (4)$$

$$X = \frac{W_{PLLA-PCL}}{W_{PLLA} + W_{PCL} + W_{PLLA-PCL}} \quad (5)$$

where, $dH_{m.PLLA}$, $dH_{c.PLLA}$, and $dH_{m.PCL}$ are the enthalpy of melting and crystallization of PLLA and PCL, respectively. 135 and 142 J/g were used as the enthalpy of fusion of PLLA and PCL crystals, respectively having infinite crystal thickness. X_{PLLA} and X are the weight fractions of PLLA and PCL/PLLA blend. W_{PLLA}, W_{PCL}, and $W_{PLLA-PCL}$ are the weights of PLLA, PCL, and PCL/PLLA blend, respectively.

Compression test and characterization of deformation mechanism

The scaffold specimens were tested under compression by using a mechanical testing machine at a displacement rate of 1 mm/min. Load–displacement curves were recorded to a computer. The compressive stress–strain curves were evaluated from the load–displacement relations. The macroscopic initial elastic modulus was calculated as the slope of the initial linear portion of the stress–strain curve. The critical stress was also evaluated at the end of the initial linear elastic portion.

The deformed scaffold specimens after the compression test were observed using FE-SEM to characterize the deformation mechanisms. The procedure of sample preparation for FE-SEM observation was the same as that described in the previous section.

Results and discussion

Porosity and microstructure

The porosities of the scaffolds estimated by Eq. 1 are shown in Fig. 2. The porosities tend to monotonically decrease with increasing PLLA content. It is known that porosity is one of the most important factor in designing scaffold for cell cultivation and a suitable porosity for cell proliferation is more than 80% [6]. Figure 2 shows that the porosities of the scaffolds were greater than 85%. The porosities are strongly related to the microstructures of the pores. Dependences of PLLA content on the average pore size and the thickness of struts surrounding the pores are shown in Fig. 3. The average pore size decreased with increasing PLLA content and hence, the corresponding strut thickness increased. Thus, the struts tend to thicken as PLLA content increased and therefore, the porosity decreased.

FE-SEM micrographs of the microstructures observed on the longitudinal (denoted as L) and the horizontal (denoted as H) cross-sections are shown in Fig. 4. Most of the scaffolds had ladder-like structures on the longitudinal sections. The ladder-like structure of the PCL scaffold was not clearly seen in Fig. 4 (a) because the struts surrounding

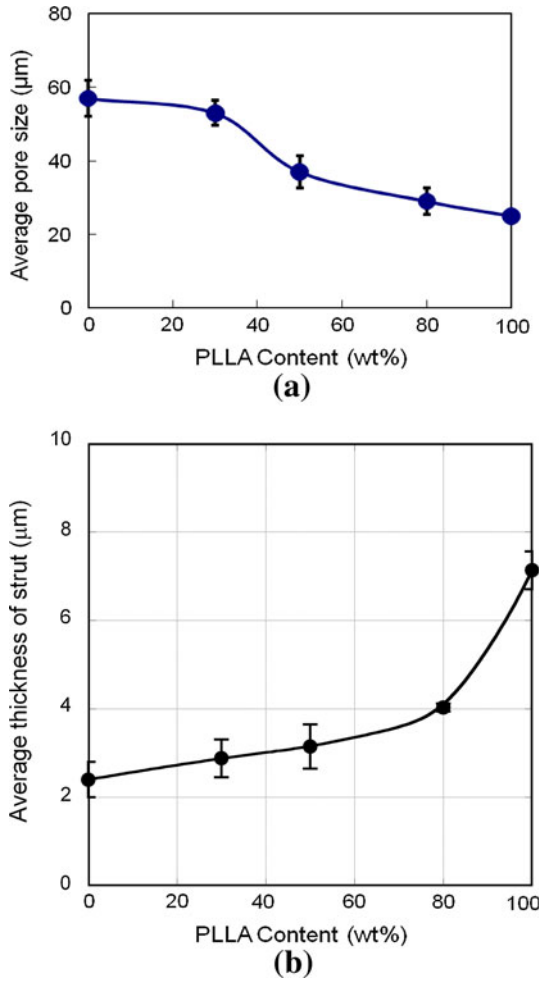

Fig. 3 Pore size and thickness of strut. **a** Average pore size, **b** Average thickness of strut

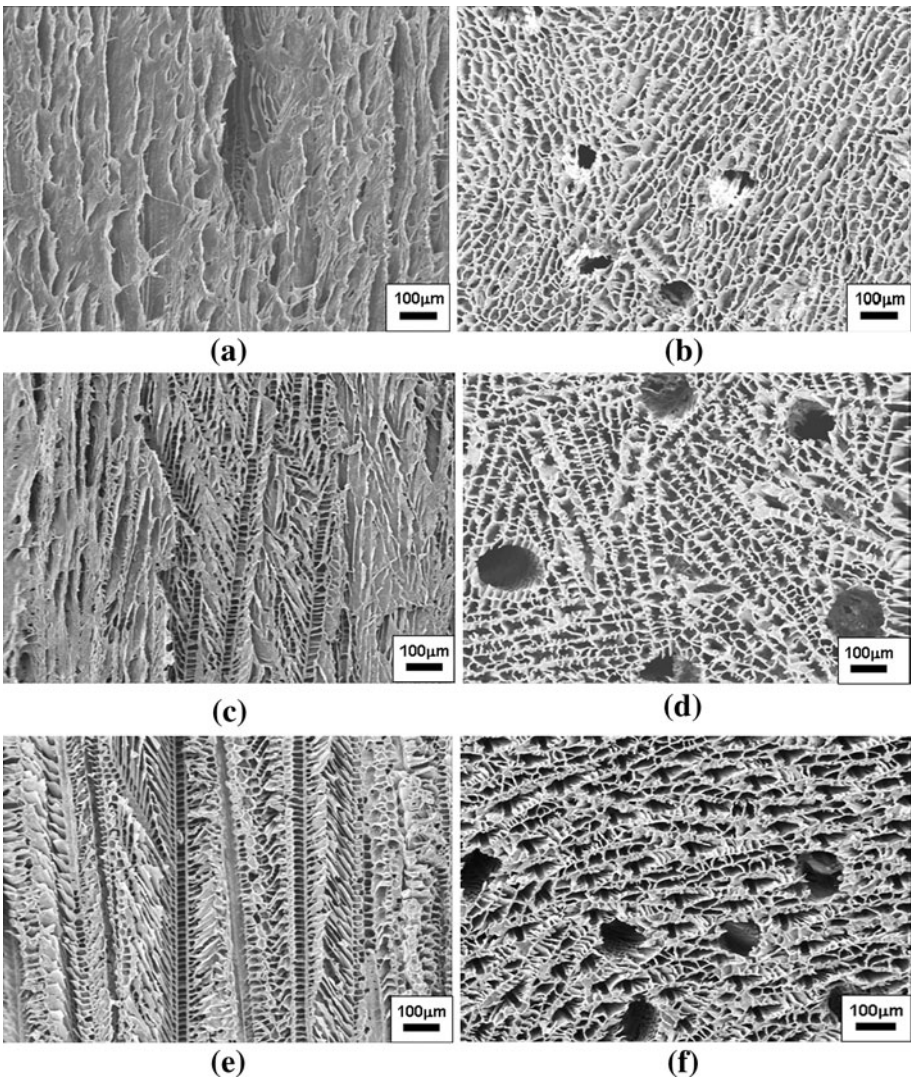

Fig. 4 Porous microstructures, **a** PCL-L, **b** PCL-H, **c** PCPL(50:50)-L, **d** PCPL(50:50)-H, **e** PLLA-L, **f** PLLA-H

the pores were plastically deformed during the cutting process. This was due to the high ductile characteristic of PCL polymer, despite the specimen being frozen in liquid nitrogen before cutting. On the other hand, homogeneous distributions of the pores are observed in the vertical cross-sections. The pores were oriented in the direction perpendicular to the cross-sections because the solvent volatilized in the same direction. The larger holes are thought to be created by solvent exhaustion.

The phase separation morphology of the PCL/PLLA blends is shown in Fig. 5. In PCPL(70:30) and PCPL(50:50), PLLA created spherical structures in the continuous domains of PCL, while in PCPL(20:80), PCL formed spherulites. The diameters of the spherulites in PCPL(70:30), PCPL(50:50), and PCPL(20:80) were roughly estimated as 300, 1000, and 500 μm, respectively. It is interesting to note that these sizes were much larger than the sizes of pores and struts as shown in Fig. 3. It is therefore, presumed that those spherulites were not formed in the porous scaffolds. Further study is needed to understand the morphology of phase separation in the PCL/PLLA blend scaffolds.

Thermal properties

The thermograms of pure PLLA and PCL, and PCPL scaffolds obtained by DSC analysis are shown in Fig. 6. The glass transition temperature, T_g, of PLLA and the melting temperature, T_m, of PCL are approximately at 64 °C, followed by the melting point of PLLA at 175 °C. In the PLLA and the PCPL samples, a peak at around 90 °C corresponds to the crystallization of PLLA. From the thermograms of PCPL, the T_m of PCL overlaps with the T_g of PLLA and therefore, two melting points exist in the PCPL scaffolds. This peculiar endothermic event in the blend is considered to be an indication that the blend

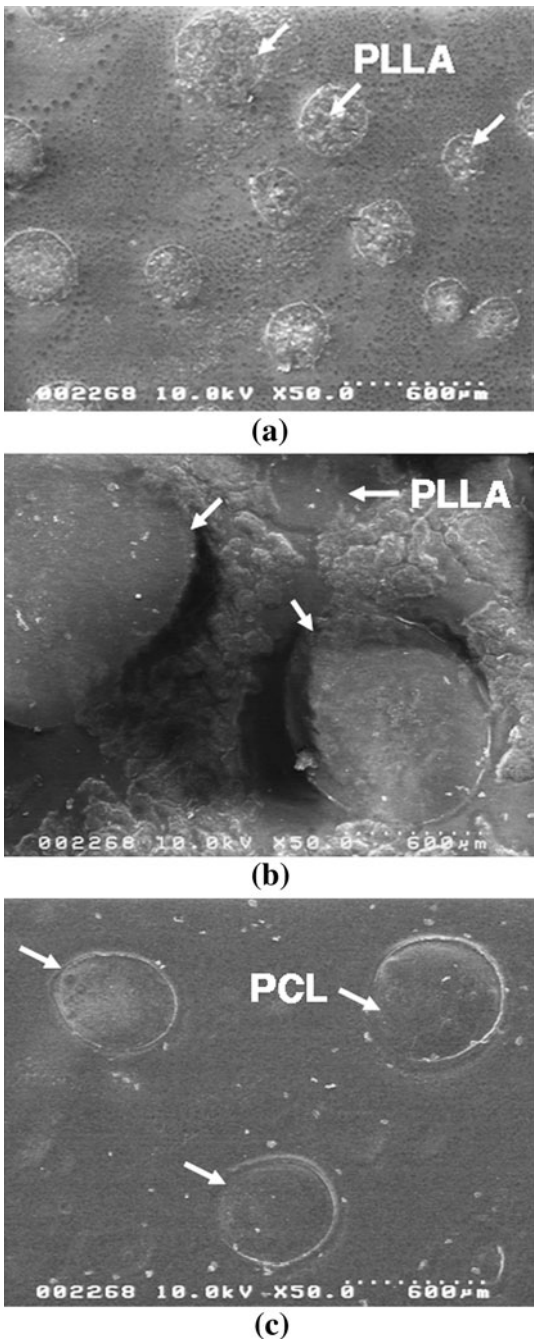

Fig. 5 Morphology of phase separation of PCL/PLLA blends made by solution casting, **a** PCPL(70:30), **b** PCPL(50:50), **c** PCPL(20:80)

scaffold has two phases in the microstructure, demonstrating the immiscibility between PCL and PLLA polymers.

Effects of PCL content on the crystallinity values of PCL and PLLA evaluated from Eqs. 2–5 are shown in Fig. 7. It can be seen that the crystallinity of PLLA tends to increase monotonically with increasing PLLA content, while the crystallinity of PCL tends to decrease as PLLA content is increased.

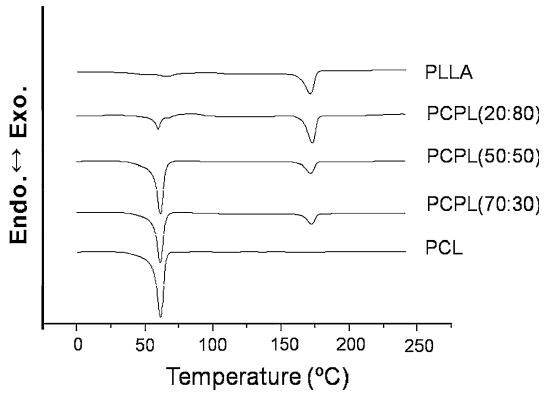

Fig. 6 Heat flow-temperature curves obtained from DSC analysis

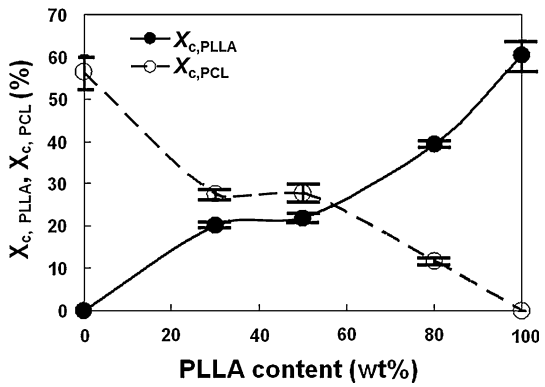

Fig. 7 Crystallinity of PLLA and PCL

Compressive mechanical properties

Typical stress–strain curves obtained from the compression tests are shown in Fig. 8. PCL showed the lowest modulus and the peak-stress, while PLLA exhibited the highest values. The modulus and the peak-stress level of the PCPL scaffolds tends to increase with increase of PLLA content. This result indicates that, the compressive mechanical properties of this kind of biodegradable polymer scaffolds can be controlled by introducing such polymer blend system of PLLA and PCL. As in our previous report [25], those stress–strain relations can be divided into two regions. The first region is recognized as the initial elastic region in which, macroscopic elastic deformation takes place. The second region is characterized as a constant or a decreasing stress region due to localized irreversible deformation under compression. In this study, the peak-stress at the transition point from the first and second regions is defined as the compressive strength since, elastic deformation collapses at this point.

The initial elastic modulus and the compressive strength are shown in Fig. 9. These compressive mechanical properties increases with increasing PLLA content.

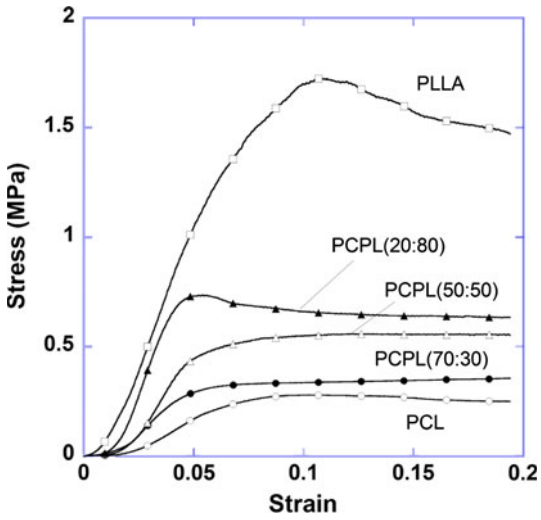

Fig. 8 Stress-strain curves under compression

The rule of mixture was used to predict those mechanical properties [28]. From this theory, mechanical properties, M, such as modulus and strength of two phase composite system, can be expressed by

$$M = V_1 M_1 + V_2 M_2 \tag{6}$$

where, V_1 and V_2 are the volume fractions of the phase 1 and 2, respectively. M_1 and M_2 are the mechanical properties of the phase 1 and 2, respectively. Equation 5 is usually valid for parallel systems in which two different phases are aligned in parallel. On the other hand, for linear systems in which two phases are aligned straight, the rule of mixture gives the following equation:

$$\frac{1}{M} = \frac{V_1}{M_1} + \frac{V_2}{M_2} \tag{7}$$

In Fig. 9a, the solid line expresses the prediction obtained by Eq. 6 and the experimental coincides with the prediction. In Fig. 9b, both the predictions by Eq. 7 (denoted by Theory A) and 6 (denoted by Theory B) are shown and the experimental coincides with Theory A. These results suggest that the elastic deformations of both PCL and PLLA phases contribute to the elastic deformation of their blends, while the compressive strength (the critical stress for the initiation of nonlinear deformation) is mainly affected by the nonlinear deformation, i.e., the plastic deformation of PCL phase. This is understood by noting that the onset of plastic deformation of PCL is much faster than that of PLLA.

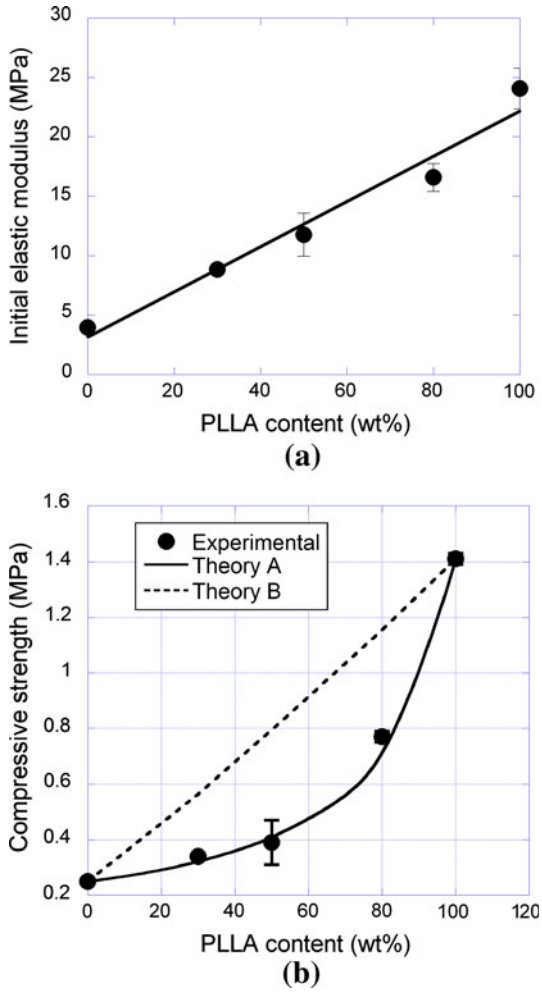

Fig. 9 Compressive mechanical properties. **a** Initial elastic modulus, **b** Compressive strength

Deformation behavior at critical point

Typical microstructural deformation behaviors observed at the critical stress points are shown in Fig. 10. The primary deformation mechanism in all the scaffolds is characterized as buckling failure of the struts surrounding the pores under compression. The PCL and PCPL scaffolds show a more defined ductile deformation behavior than the PLLA, and the deformation regions are much wider as well. The right-hand figures exhibit the deformation micromechanisms in these scaffolds. Pure PCL showed very ductile deformation with formation of elongated fibrils. On the contrary, PLLA exhibited the collapse of the struts with localized plastic deformation. In the PCPL scaffold, elongated holes are observed and these are thought to be the interfacial failure between the PCL and PLLA phases or the tearing failure within the PCL phases. This kind of failure mode corresponds to the immiscibility of PCL and PLLA. This immiscibility result in generating phase separation morphology on the surface of the polymer blend due to the difference of chemical structures [29–31].

Conclusions

Biodegradable PCL/PLLA polymer blend scaffolds were successfully developed by using the solid–liquid phase separation method and subsequent freeze-drying method. Porous structures and thermal properties of the blend system were examined and the compressive mechanical testing was also performed to assess the effects of blend ratio on the mechanical properties. Microscopic deformation behaviors of the scaffolds were also examined using FE-SEM. The results obtained are as follows:

(1) Porosity of PCL/PLLA scaffold tends to decrease with increasing PLLA content. This is because the struts surrounding the pores tend to thicken as PLLA content increases and therefore, the average size of pores becomes smaller, resulting in the decrease in porosity.

(2) The compressive mechanical properties, such as the initial elastic modulus and the compressive strength, increase with increasing PLLA content. The modulus can be well predicted by the parallel model derived from the rule of mixture. On the contrary, the linear line model can be used to predict the compressive strength.

(3) The primary deformation mechanism of all the scaffolds is localized buckling of the struts with plastic deformation. The ductility of the struts decreases with increasing PLLA content, resulting in increase of the modulus and the compressive strength.

(4) The results of DSC analysis and the microstructural observation indicated the phase separation morphology of the blend system caused by the immiscibility of PCL and PLLA. This kind of phase separation greatly affects both the macroscopic mechanical

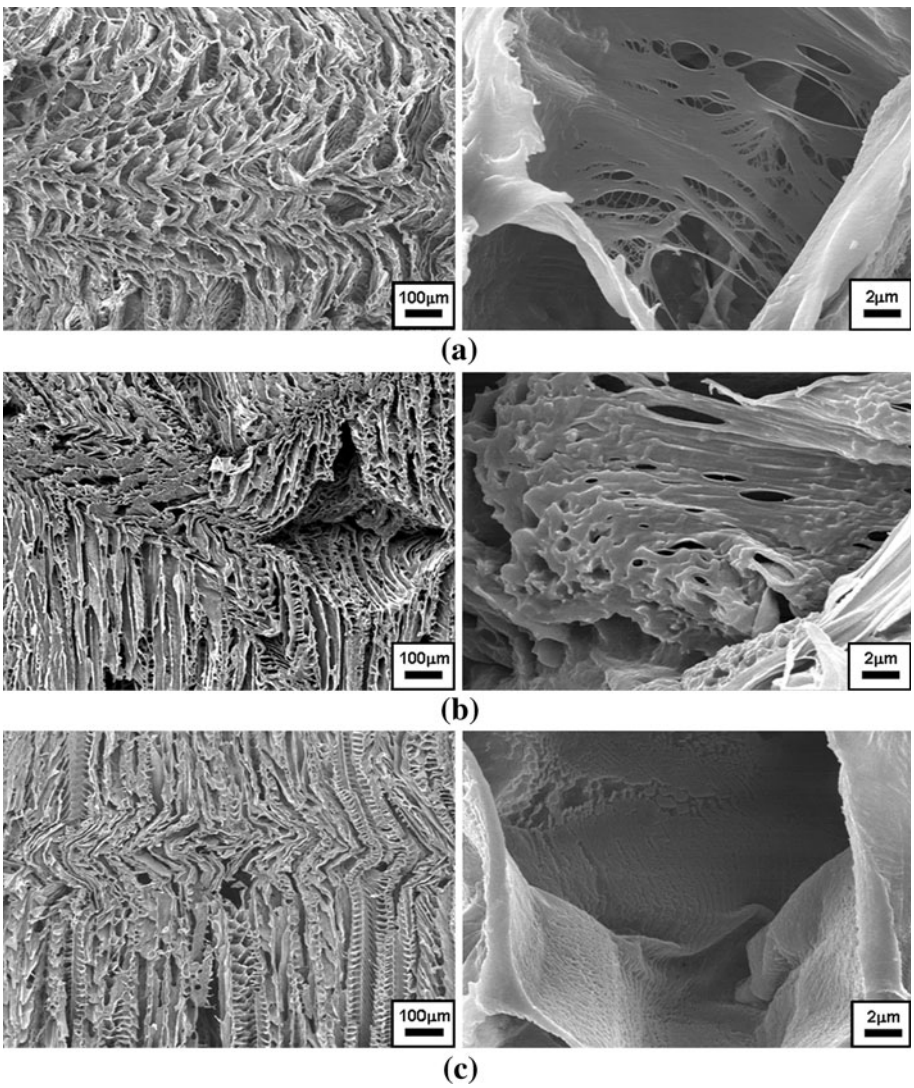

Fig. 10 Deformation behavior at critical stress, **a** PCL, **b** PCPL (50:50), **c** PLLA

properties and the microscopic deformation behavior of the blend scaffolds.

References

1. Roosa SMM, Kemppainen JM, Moffitt EN, Krebsbach PH, Hollister SJ (2009) J Biomed Mater Res 92A:359
2. Zhou WY, Lee SH, Wang M, Cheung WL, Ip WY (2008) J Mater Sci Mater Med 19:2535
3. Shimko DA, Shimko VF, Sander EA, Dickson KF, Nauman EA (2005) J Biomed Mater Res 73B:315
4. Wu L, Ding J (2005) J Biomed Mater Res 75A:767
5. Hou Q, Grijpma DW, Feijen J (2003) Biomaterials 24:1937
6. Li X, Feng Q, Cui F (2006) Mater Sci Eng 26C:716
7. Georgiou G, Mathieu L, Pioletti DP, Bourban PE, Manson JAE, Knowles JC, Nazhat SN (2007) J Biomed Mater Res 80B:322
8. Barry RA III, Shepherd RF, Hanson JN, Nuzzo RG, Wiltzius P, Lewis JA (2009) Advan Mater 21:2407
9. Kang HW, Rhie JW, Cho DW (2009) Microelec Eng 86:941
10. Michna S, Wu W, Lewis JA (2005) Biomaterials 26:5632
11. Leukers B, Gülkan H, Irsen SH, Milz S, Tille C, Schieker M, Seitz H (2005) J Mater Sci Mater Med 16:1121
12. Dellinger JG, Eurell JAC, Jamison RD (2005) J Biomed Mater Res 76A:366
13. Mikos AG, Thorsen AJ, Czerwonka LA, Bao Y, Langer R (1994) Polymer 35:1068
14. Zhang R, Ma PX (1999) J Biomed Mater Res 45:285
15. Zhang R, Ma PX (1999) J Biomed Mater Res 44:446
16. Oh SH, Park IK, Kim JM, Lee JH (2007) Biomaterials 28:1664
17. Li WJ, Danielson KG, Alexander PG, Tuan RS (2003) J Biomed Mater Res 67A:1105
18. Kim SS, Park MS, Jeon OJ, Choi CY, Kim BS (2006) Biomaterials 27:1399
19. Wei G, Ma PX (2004) Biomaterials 25:4749
20. Zhang P, Hong Z, Yu T, Chen X, Jing X (2009) Biomaterials 30:58
21. Kang Y, Yin G, Yuan Q, Yao Y, Huang Z, Liao X, Yang B, Liao L, Wang H (2008) Mater Lett 62:12
22. Todo M, Park SD, Takayama T, Arakawa K (2007) Eng Fract Mech 74:1872
23. Todo M, Park JE, Kuraoka H, Kim JW, Taki K, Ohshima M (2009) J Mater Sci 44:4191. doi:10.1007/s10853-009-3546-0
24. Den Dunnen WFA, Schakenraad JM, Zondervan GJ, Pennings AJ, Van Der Lei B, Robinson PH (1993) J Mater Sci Mater Med 4:521
25. Todo M, Kuraoka H, Kim JW, Taki K, Ohshima M (2008) J Mater Sci 43:5644. doi:10.1007/s10853-008-2881-x
26. Tu C, Cai Q, Yang J, Wan Y, Bei J, Wang S (2003) Polym Advan Tech 14:565
27. Tsuji H, Yamada T, Suzuki M, Itsuno S (2003) Polym Int 52:269
28. Nielsen LE (1975) Marcel Dekker, Inc., New York
29. Chen CC, Chueh JY, Tseng H, Huang HM, Lee SY (2003) Biomaterial 24:1167
30. Takayama T, Todo M (2006) J Mater Sci 41:4989. doi:10.1007/s10853-006-0137-1
31. Na YH, He Y, Shuai X, Kikkawa Y, Doi Y, Inoue Y (2002) Biomacromolecules 3:1179